

# Molecular resonant dissociation of surface-adsorbed molecules by plasmonic nanoscissors†

Cite this: *Nanoscale*, 2014, 6, 4903Zhenglong Zhang,<sup>abc</sup> Shaoxiang Sheng,<sup>a</sup> Hairong Zheng,<sup>b</sup> Hongxing Xu<sup>a</sup> and Mengtao Sun<sup>\*a</sup>

The ability to break individual bonds or specific modes in chemical reactions is an ardently sought goal by chemists and physicists. While photochemistry based methodologies are very successful in controlling e.g. photocatalysis, photosynthesis and the degradation of plastic, it is hard to break individual molecular bonds for those molecules adsorbed on the surface because of the weak light-absorption in molecules and the redistribution of the resulting vibrational energy both inside the molecule and to its surrounding environment. Here we show how to overcome these obstacles with a plasmonic hot-electron mediated process and demonstrate a new method that allows the sensitive control of resonant dissociation of surface-adsorbed molecules by 'plasmonic' scissors. To that end, we used a high-vacuum tip-enhanced Raman spectroscopy (HV-TERS) setup to dissociate resonantly excited NC<sub>2</sub>H<sub>6</sub> fragments from Malachite green. The surface plasmons (SPs) excited at the sharp metal tip not only enhance the local electric field to harvest the light incident from the laser, but crucially supply 'hot electrons' whose energy can be transferred to individual bonds. These processes are resonant Raman, which result in some active chemical bonds and then weaken these bonds, followed by dumping in lots of indiscriminant energy and breaking the weakest bond. The method allows for sensitive control of both the rate and probability of dissociation through their dependence on the density of hot electrons, which can be manipulated by tuning the laser intensity or tunneling current/bias voltage in the HV-TERS setup, respectively. The concepts of plasmonic scissors open up new versatile avenues for the deep understanding of *in situ* surface-catalyzed chemistry.

Received 23rd December 2013  
Accepted 19th February 2014

DOI: 10.1039/c3nr06799h

www.rsc.org/nanoscale

## 1 Introduction

Developing methodologies that enable mode-specificity chemistry is a very important goal for chemists and an active field of study in the area of molecular reaction dynamics.<sup>1,2</sup> One promising avenue for realizing vibration-resolved resonant dissociation relies on the excitation and control of molecular vibrations. However, controlling vibrational modes for chemical reactions is challenging because of intramolecular vibrational energy redistribution<sup>1,3</sup> (IVR) within an excited molecule on a picosecond time scale. For molecules in a gas, bond-breaking of molecular bonds can be induced and controlled by feedback-optimized phase-shaped femtosecond laser pulses.<sup>2</sup> But for surface-adsorbed molecules the situation is significantly complicated by the dissipation of energy to the surrounding

surface atoms, which take up the energy and thwart the bond-breaking process. Recent efforts have tried to address this issue by using a laser to vibrationally excite C–H bonds in a gas-phase beam of triply deuterated methane molecules in such a way that the C–H bonds would break as the molecules glance off a metal surface.<sup>4</sup> However, the challenge still remains as to how to achieve efficient, resonance excitation by laser and dissociation by hot electrons for molecules adsorbed on a solid surface, prior to the time scale of IVR, and energetic redistribution between the adsorbates and their environment. Vibrational mode specific bond dissociation in a single molecule has been performed by tunneling electrons from a scanning tunneling microscope (STM),<sup>5,6</sup> but we herein focus on the plasmon-driven resonantly excited vibration-resolved resonant dissociations by plasmonic hot electrons as plasmonic scissors in STM-based tip-enhanced Raman spectroscopy (TERS).

Recent reports have shown that hot electrons generated from plasmon decay (Landau damping)<sup>7–9</sup> can play an important role in surface chemical reactions.<sup>9–17</sup> Very recently, surface catalytic reactions in TERS have been expected,<sup>16,18,19</sup> and the molecular dimerization in TERS has been successfully realized experimentally. Plasmon scissors for molecular designs have been reported in TERS and SERS experiments,<sup>20,21</sup> where hot electrons (generated

<sup>a</sup>Beijing National Laboratory for Condensed Matter Physics, Institute of Physics, Chinese Academy of Sciences, P. O. Box 603-146, Beijing, 100190, People's Republic of China. E-mail: mtsun@iphy.ac.cn

<sup>b</sup>School of Physics and Information Technology, Shaanxi Normal University, Xi'an, 710062, People's Republic of China

<sup>c</sup>Leibniz Institute of Photonic Technology, Albert-Einstein-Str. 9, 07745, Jena, Germany

† Electronic supplementary information (ESI) available: Further experimental spectra and theoretical calculations. See DOI: 10.1039/c3nr06799h

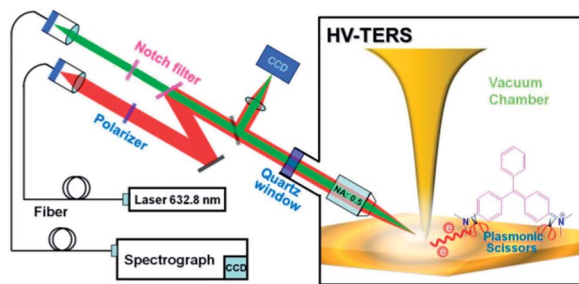


Fig. 1 Home-made setup of high-vacuum tip-enhanced Raman spectroscopy (HV-TERS) and mechanism of resonant dissociation by plasmonic scissors. Hot electrons are excited by laser light in the nanogap of a TERS setup to cut molecular bonds in the substrate-adsorbed Malachite green molecules.

from plasmon decay) break the weakest  $-N=N-$  bond of DMAB, while the Raman spectra were not bond-selectively resonant excited (they are normal Raman). Recently, the concept of plasmon-driven selective bond activation has been proposed.<sup>22,23</sup> The hot electrons transfer energy to molecules adsorbed on the substrate, and thereby induced electron-driven bond dissociation.<sup>22,23</sup> Firstly, hot electrons are attached temporarily to the PES of molecules, which transiently charges the neutral PES to negative PES and decreases the reaction barrier. Secondly, the reaction energy can be excited to be higher than or close to the dissociation energy using a laser. Then, the high kinetic energy of the hot electrons provides the additional energy required for dissociation of the active bonds.<sup>11,17,20,22,23</sup> Here we show how hot electrons generated from the plasmon decay in the nanogap of a high-vacuum TERS (HV-TERS) setup (see Fig. 1) can be used to dissociate the resonantly excited Malachite Green (MG) adsorbed on Ag and Au surfaces with sensitive control of the dissociation rate and probability through tuning of the hot electron density. These processes are resonant Raman to active some chemical bonds and then weaken these bonds, followed by dumping in lots of indiscriminant energy and breaking of the weakest bond.

The method relies on the hot electrons and laser signal working in tandem. The laser assists to resonantly excite electronic transitions in molecular bonds in the MG. The hot electrons in turn provide the required energy to significantly overcome the reaction barrier and trigger the chemical reaction.<sup>11,16,17,20,22,23</sup> Importantly, the lifetime of the hot electrons is on the order of femtoseconds, which is much shorter than the picosecond time scale of IVR. Furthermore, because the density of the hot electrons can be rationally controlled, *via* for example tuning of the laser signal, our methodology offers control of the rate and probability of the chemical reaction. Note that our resonant dissociative method relies on optical, rather than electrical means, as is the case in STM-related control of chemical reactions.<sup>5,6</sup>

## 2 Experimental and theoretical methods

Vibrational spectra were recorded with a home-built HV-TERS setup.<sup>24–26</sup> It consists of a homemade scanning tunneling

microscope (STM) in a high vacuum chamber, a Raman spectrometer combined with a side illumination of 632.8 nm He-Ne laser light with an angle of  $30^\circ$  for Raman measurements, and three-dimensional piezo stages for the tip and sample manipulations. The objective is placed in the high vacuum chamber. The pressure in the chamber is about  $10^{-7}$  Pa. A gold tip with a radius of about 50 nm was prepared by electrochemical etching of a 0.25 mm diameter gold wire.<sup>27</sup> The substrate was prepared by evaporating a 100 nm silver film to a newly cleaned mica film under high vacuum. The film was immersed in  $1 \times 10^{-5}$  M MG in ethanol solution for 24 hours, respectively, and then washed with ethanol for 10 minutes to guarantee that there was only one monolayer of molecules adsorbed on the silver film. Then the sample was immediately put into the high vacuum chamber. To get a good signal-to-noise ratio, the TERS signals were collected with an acquisition time of 20 seconds and accumulated 10 times for each spectrum on the Ag film and 40 seconds and accumulated 20 times for each spectrum on the Au film. We also recorded the absorption spectrum of MG  $10^{-2}$  M in water with absorption spectroscopy (Hitachi U3010). SERS and SERRS spectra of MG were recorded in Ag sol, using Leica microscopy equipment in a confocal Raman spectroscopic system (Renishaw, Invia), and the incident wavelengths are 785, 632.8 and 514.5 nm. The Ag sol for SERS measurement was synthesized, using Lee's method,<sup>28</sup> and the average diameter of nanoparticles is 80 nm.<sup>10</sup>

The theoretical simulations on Raman spectra were performed, using density functional theory,<sup>29</sup> B3LYP functional,<sup>30,31</sup> 6-31G(d) basis for C, N, H atoms, and LANL2DZ basis<sup>32</sup> for Ag atoms, which were implemented in Gaussian 09.<sup>33</sup> These theoretical methods have been used to investigate Raman spectra in the HV-TERS system, which are rational theoretical methods.<sup>24</sup>

## 3 Results and discussion

The demonstration of the resonant dissociation of MG relies on several complementary experimental and theoretical investigations. Firstly, we measured the optical absorption spectrum of MG (see Fig. 2a), which revealed that there is no absorption peak at 785 nm, but there is a strong absorption peak around 632.8 nm, and a very weak absorption peak at 514.5 nm. Secondly, SERS spectra of MG in Ag sol were recorded at these three frequencies (see Fig. 2b). It is normal Raman excited at 785 nm, and the Raman excited one at 514 nm is similar to that excited at 785 nm; while it is resonance Raman excited at 632.8 nm, where Raman peaks A–D are selectively excited by resonance electronic transition at 632.8 nm, when peak E is considered the normalized peak for comparison (the figures of Raman spectra without normalization can be seen from Fig. S1(a) in the ESI†). Thirdly, our theoretical calculations identify that peaks A–D related to vibrational modes in MG are associated with the  $-NC_2H_6$  fragments (Fig. 2c). MG exhibits  $C_2$  symmetry, and there are two kinds of vibrational modes a and b, and these five selectively enhanced vibrational modes were assigned as  $a_{39}$ ,  $a_{45}$ ,  $b_{49}$ ,  $b_{61}$  and  $a_{58}$  from low to high frequencies. The simulated normal Raman spectrum of MG can be seen

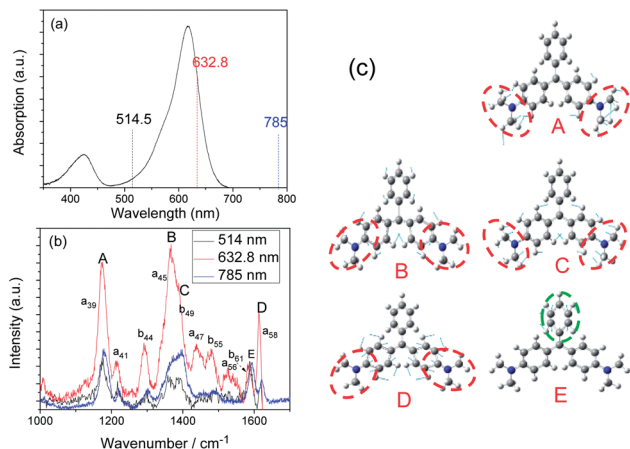


Fig. 2 Absorption and Raman spectra and calculated normal modes of MG. (a) Absorption spectrum of MG in water, (b) SERS and SERRS spectra of MG in Ag sol, and (c) vibrational modes A–E of MG.

from Fig. S1(b),† and the assignments of the normal Raman spectrum are listed in Table S1 in the ESI.†

Peak E in Fig. 2b on the other hand is a vibrational mode associated with the C–C stretching mode of benzenyl. Consequently, our analysis shows that the energy of resonant excitation at 632.8 nm is concentrated on modes A–D related to the  $-\text{NC}_2\text{H}_6$  fragments. These modes can thus be selectively resonant excited. Note that peaks B and C in Fig. 2b were superposed due to a wide half high width, but they are well separated in HV-TERRS in Fig. 3a. By comparing TERRS excited at 632.8 nm and SERS excited at 785 nm, it is very clear that peaks A–D were selectively excited (see Fig. S1(c)†).

Now, we demonstrate the resonant dissociation process through time-dependent measurements using tip-enhanced resonance Raman spectroscopy (TERRS) in high vacuum at the incident light of 632.8 nm. Fig. 3a–c are time-sequential TERRS of MG adsorbed on the Ag surface in high-vacuum in the presence of the incident light at 632.8 nm. At the initial stage, when the laser just radiates on the sample ( $t = 0$  minutes), the measured TERRS spectrum (Fig. 3a) shows that the Raman peaks A–D are strongly enhanced in TERRS by comparing with the off-resonance SERS spectrum excited at 785 nm (see Fig. S1(b) in ESI†), where the Raman peak E at  $1592\text{ cm}^{-1}$  is used as the normalized peak in comparison. This means that the resonant excitation energies mainly selectively excite these four vibrational modes during the electronic transition. Our time-sequential TERRS measurements show evidence of a time-dependent molecular reaction dynamics process (Fig. 3a–c) that leads to a suppression of peaks A–D and the emergence of new ones over time. Keeping the laser beam intensity constant over a period of time yields, at first, an increasingly complex and unstable vibrational spectrum (Fig. 3b). After a period of 40 minutes the spectrum stabilizes into the configuration shown in Fig. 2c. Strongly enhanced Raman peaks A–D that were initially present (Fig. 3a) are now not visible, whereas new peaks (denoted F–M in Fig. 3c) have emerged. The 2D plot of TER spectra (see Fig. 4) revealed that Fig. 3c is the stable final spectra

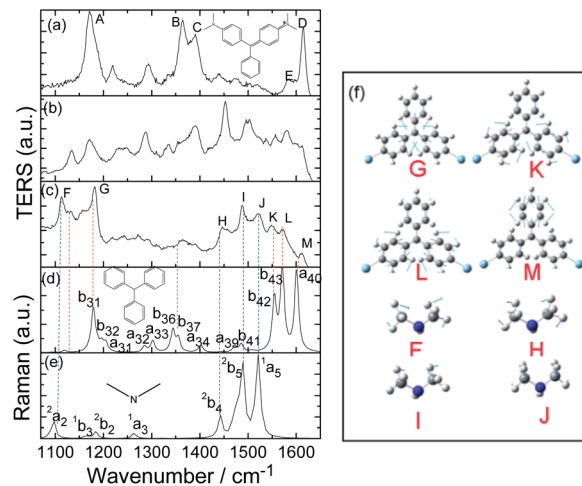


Fig. 3 Time sequential TERRS and the vibrational modes of MG. (a) The initial, (b) intermediate (20 minutes after continuous radiation using a laser), and (c) the final spectra (40 minutes after continuous radiation using a laser). The tunneling current and the bias voltage are 1 nA and 1 V, respectively. (d and e) Simulated Raman spectra of fragments (see the insets). (f) The vibrational modes of dissociated fragments of MG (corresponding to the experimental peaks in (d) and (e) as calculated by density functional theory).

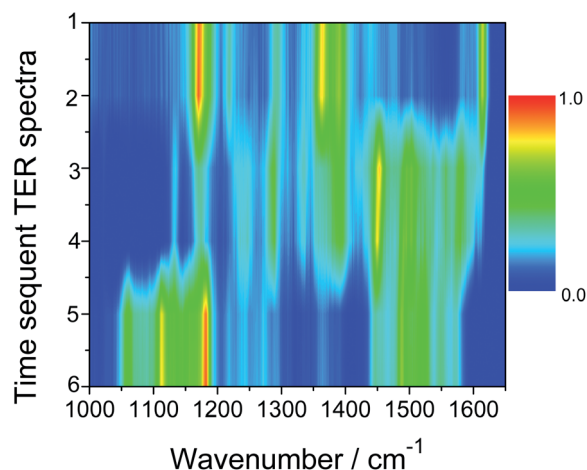


Fig. 4 Time sequential TER spectra, and the color bar is shown in the right of the figure. The time interval is 20 minutes for each TER spectrum.

under our experimental conditions. Fig. 3d and e are the simulated Raman spectra of dissociated fragments from MG, and their vibrational modes were also assignments, which can also be seen from Tables S2 and S3 in the ESI.† The fragment of  $\text{HN}(\text{CH}_3)$  exhibits  $C_{2v}$  symmetry; there are four kinds of vibrational modes,  $a_1$ ,  $a_2$ ,  $b_1$  and  $b_2$ . The large fragment in Fig. 3d exhibits  $D_3$  symmetry, while when it is attached to a metal (see Fig. 3f), it exhibits  $C_2$  symmetry, and two kinds of vibrational modes a and b. Their vibrational modes were also assigned in Fig. 3d and e. The vibrational modes F–M in Fig. 3c can be seen from Fig. 3f. The time-evolution of the TERRS spectra in Fig. 3 provides evidence for a dissociative chemical reaction taking

place in MG. As the simulations of Raman spectra of the fragments of dissociation (Fig. 3d and e) clearly show, the final TERS spectrum in Fig. 3c contains signatures from both dissociated fragments. It is important to estimate the ratio of chemical reactions in HV-TERS. There are about 157 molecules under the tip before reaction within an effective  $78 \text{ nm}^2$  area (see discussion and Fig. S2 in ESI†), where the size of every molecule is about  $0.5 \text{ nm}^2$ . By comparing the intensity of peak C in Fig. 3a and c, more than 60% of them have been dissociated by plasmon scissors. Also, by comparing the ratio of intensities of experimental and theoretical Raman peaks of G and I in Fig. 3c, more than 40% molecules of  $\text{N}(\text{CH}_3)_2$  are still present (another 20% molecules of  $\text{N}(\text{CH}_3)_2$  were desorbed and pumped out of the high vacuum chamber).

We also made similar observations also for MG adsorbed on the Au film (see Fig. 5). Note that Fig. S2 in the ESI,† which is also measured after 40 minutes, similar to the results shown in Fig. 3b, displays evidence of a partial reaction since peaks A–C are not completely vanished yet compared to Fig. 3c, even though the new peaks F–M have appeared. We therefore conclude that the chemical reaction on the Au substrate is slower than that on the Ag film.

Note that we believe the process of electron transfer should be in the time scale of femtoseconds, if hot electrons have successfully attached to molecules. While, there is a probability that how many hot electrons can successfully attach to molecules, which strongly depends on the density of electrons. The plasmon intensity along the substrate is highly asymmetric;

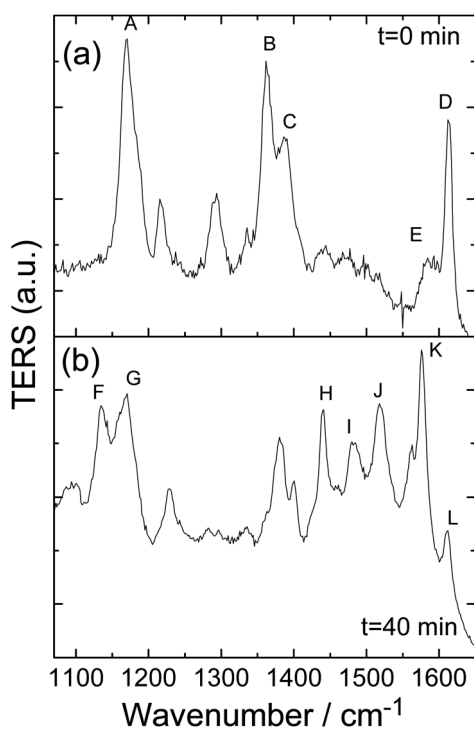


Fig. 5 Time sequential TERS and the vibrational modes of MG adsorbed on the Au film. (a) The initial and (b) the spectra at 40 minutes after continuous radiation using a laser. The tunneling current and the bias voltage are 1 nA and 1 V, respectively.

when away from the center, the plasmon intensity is weaker. So, the reaction region of all molecules within effective  $78 \text{ nm}^2$  (see ESI†) in the effect region is not simultaneously. Very far from the center, the plasmon intensity is weak, and then the density of hot electrons is weaker. So, the probability of electrons successfully attached to molecules is also smaller, compared with the reaction at the center of gap, and therefore, the chemical reactions are slower than those at the center of the nanogap.

The rate and probability of chemical reactions can be controlled by varying the tunneling current, bias voltage and laser intensity in HV-TERS. In our method, the most natural way of controlling the rate and probability of dissociation is by changing the plasmon intensity *via* tuning of the laser intensity.<sup>16</sup> As demonstrated in Fig. 6a and b, a decrease of the laser power by 10% of the total laser power yields a much slower dissociation rate – after 40 minutes, the spectra shown in Fig. 6d show the strongly enhanced Raman peaks A–C were still visible, though new peaks have emerged (see Fig. 6b).

To elucidate the origin of the observed dissociation, we have performed additional measurements to evaluate the contribution of the tunneling current to the resonant dissociation process. Previous reports have shown that chemical bonds can be broken or formed by tunneling electron currents or bias voltages alone.<sup>5,6,34,35</sup> Our measurements and analyses show that this is not the case in our study measurements of TERS spectra at  $t = 0$  and  $t = 40$  minutes, without the irradiation of the sample using laser light there between, and at a constant tunneling current, show that the profiles of the two TERS spectra are identical (see Fig. 6c–d). Consequently, the energy provided by the laser and the tunneling current is not large enough to dissociate the molecules, unless the laser continuously irradiates the sample to provide a continuous supply of a large density of hot electrons.

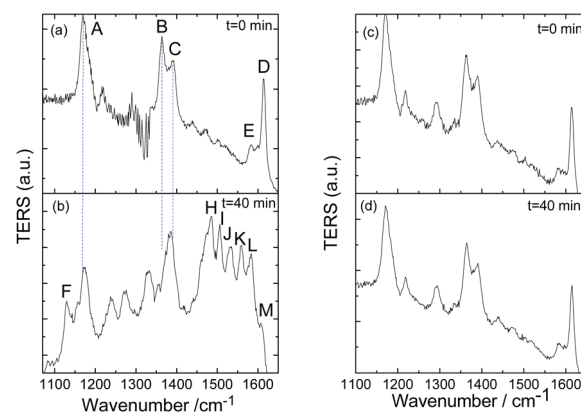


Fig. 6 TERS of MG adsorbed on the Ag film at  $t = 0$  and  $t = 40$  minutes. (a and b) Sample irradiated with 10% lower laser power compared to the sample analyzed in Fig. 2a and c shows evidence for a slower dissociation rate and, (c)–(d) without continuous laser-irradiation of the sample shows that the tunneling current alone is not sufficient to induce dissociation.

The physical origins of the resonant dissociation rely on the generation of hot electrons. Large densities of plasmons are first produced by the laser irradiation of the nanogap between the tip and substrate in the HV-TERS. Hot electrons with high kinetic energy are then generated from the plasmon decay and work in tandem with the laser beam to induce the dissociation process (see Fig. 7). The resonant electronic transition increases the lifetime of the Raman scattering (compared to the normal Raman scattering) and the resonant excitation by the laser results in the excitation energy concentrating on the vibrational modes associated with the  $-\text{NC}_2\text{H}_6$  fragments of MG, thereby selectively weakening these bonds (process A in Fig. 7). The hot electrons generated from the plasmon decay in turn serve two purposes: first, because of their high kinetic energy, when the hot electrons impinge on the metal-adsorbed molecules, they induce a change of the molecule excited-state potential energy surface (ESPES) from a neutral to a temporarily negative ion excited state (ESPES<sup>-</sup>) (process B in Fig. 7). The redox state due to the hot electron is a transient negative state.<sup>36</sup>

Second, the kinetic energy is transferred from the hot electrons to the intra-molecular vibrational dissociation energy during their interactions (process C in Fig. 7). Both of these processes lead to an effective overcoming of the energy barrier (Fig. 7) for the chemical reaction to take place – either by overcoming or tunneling through the barrier such that the reaction leading to dissociation can occur. Note that in our experiment, to keep stable the B and C components of the total energy required by the chemical reaction, we have to irradiate the sample continuously by the laser to sustain a large density of hot electrons. It is a multi-electron driven process. Note that hot electrons donating their energy to the molecule are not necessarily bond-selective. In short, this process shown in Fig. 7 is resonant Raman to selectively weaken the bond, followed by dumping in lots of indiscriminant energy and breaking these active weakest bonds. So, the bond broken is not simply the lowest energy one available, but actually was induced selectively.

Furthermore, the laser intensity, tunneling current or bias voltage in the HV-TERS may also provide further energy for the

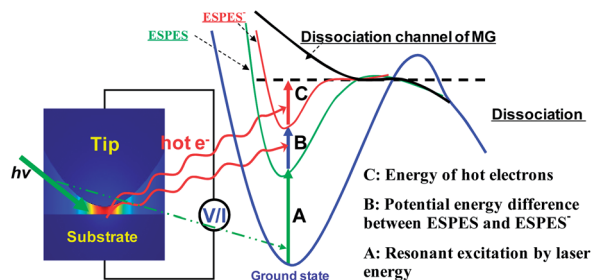


Fig. 7 The mechanism of resonant dissociation by plasmon scissors. Three main energetic components drive the chemical reaction: (A) resonant absorption of the laser light enhances the vibrational modes associated with  $-\text{NC}_2\text{H}_6$  and excites the MG molecules to an excited-state potential energy surface (ESPES); (B) hot electrons temporarily change the molecules' ESPES from a neutral to a negative ion excited state (ESPES<sup>-</sup>); (C) the kinetic energy of the hot electrons is converted into intramolecular vibrational thermal energy.

dissociation. This allows for control of the rate and probability of dissociation. As shown in Fig. 6, decreasing the laser intensity leads to a slower dissociation rate and probability. This is because the decrease in the laser intensity leads to a decrease in the plasmon intensity, which in turn determines the density of hot electrons. It should be noted that the diagram in Fig. 7 is qualitative. The energy of hot electrons generated from plasmon decay may be less than that of photons, if these hot electrons relaxed before reacting; otherwise, it is just as large as the photons as well.

## 4 Conclusion

In conclusion, our study not only demonstrates the plasmonic scissor concept as an efficient tool for resonant control of dissociation of surface-adsorbed molecules, but establishes the concept of plasmonic hot-electron mediated chemistry as an important new field extending the reach of photochemistry to chemical reactions where simple photon absorption does not suffice, but where the additional energy supplied by hot electrons generated by SPs yields the necessary means of control. It also demonstrates that HV-TERS is a promising technique for *in situ* surface chemical analysis and manipulation on the nanoscale.

## Acknowledgements

This work was supported by the National Natural Science Foundation of China (grants 11374353, 11274149 and 11174190) and the Program of Shenyang Key Laboratory of Optoelectronic Materials and Technology (F12-254-1-00).

## References

- 1 F. F. Crim, *Proc. Natl. Acad. Sci. U. S. A.*, 2008, **105**, 12654–12661.
- 2 A. Assion, T. Baumert, M. Bergt, T. Brixner, B. Kiefer, V. Seyfried, M. Strehle and G. Gerber, *Science*, 1998, **282**, 919–922.
- 3 T. Uzer and W. H. Miller, *Phys. Rep.*, 1991, **199**, 73–146.
- 4 D. R. Killelea, V. L. Campbell, N. S. Shuman and A. L. Utz, *Science*, 2008, **319**, 790–793.
- 5 J. R. Hahn and W. Ho, *J. Chem. Phys.*, 2009, **131**, 044706, (1–4).
- 6 Y. Jiang, Q. Huan, L. Fabris, G. C. Bazan and W. Ho, *Nat. Chem.*, 2013, **5**, 36–41.
- 7 M. W. Knight, H. Sobhani, P. Nordlander and N. J. Halas, *Science*, 2011, **332**, 702–704.
- 8 (a) Z. L. Zhang, L. Chen, M. T. Sun, P. P. Ruan, H. R. Zheng and H. X. Xu, *Nanoscale*, 2013, **5**, 3249; (b) Z. L. Zhang, M. T. Sun, P. P. Ruan, H. R. Zheng and H. X. Xu, *Nanoscale*, 2013, **5**, 4151.
- 9 K. Watanabe, D. Menzel, N. Niluis and H. J. Freund, *Chem. Rev.*, 2006, **106**, 4301–4320.
- 10 Y. R. Fang, Y. Z. Li, H. X. Xu and M. T. Sun, *Langmuir*, 2010, **26**, 7737–7746.
- 11 P. Christopher, H. L. Xin and S. Linic, *Nat. Chem.*, 2011, **3**, 467–472.

- 12 S. Linic, P. Christopher and D. B. Ingram, *Nat. Mater.*, 2011, **10**, 911–921.
- 13 H. P. Zhu, G. K. Liu, D. Y. Wu, B. Ren and Z. Q. Tian, *J. Am. Chem. Soc.*, 2010, **132**, 9244–9246.
- 14 (a) M. T. Sun and H. X. Xu, *Small*, 2012, **8**, 2777–2786; (b) M. T. Sun, Z. L. Zhang, P. J. Wang, Q. Li, F. C. Ma and H. X. Xu, *Light: Sci. Appl.*, 2013, **2**, e112.
- 15 L. Brus, *Acc. Chem. Res.*, 2008, **41**, 1742–1749.
- 16 (a) M. T. Sun, Z. L. Zhang, H. R. Zheng and H. X. Xu, *Sci. Rep.*, 2012, **2**, 647, (1–4); (b) M. T. Sun, Y. R. Fang, Z. Y. Zhang and H. X. Xu, *Phys. Rev. E: Stat., Nonlinear, Soft Matter Phys.*, 2013, **87**, 020401.
- 17 S. Mukherjee, F. Libisch, N. Large, O. Neumann, L. V. Brown, J. Cheng, J. B. Lassiter, E. A. Carter, P. Nordlander and N. J. Halas, *Nano Lett.*, 2013, **13**, 240–247.
- 18 H. Kim, K. M. Kosuda, R. P. Van Duyne and P. C. Stair, *Chem. Soc. Rev.*, 2010, **39**, 4820–4844.
- 19 E. M. V. Lantman, T. Deckert-Gaudig, A. J. G. Mank, V. Deckert and B. M. Weckhuysen, *Nat. Nanotechnol.*, 2012, **7**, 583–586.
- 20 M. T. Sun, Z. L. Zhang, Z. H. Kim, H. R. Zheng and H. X. Xu, *Chem. - Eur. J.*, 2013, **19**, 14958.
- 21 K. Kim, K. L. Kim and K. S. Shin, *Langmuir*, 2013, **29**, 183–190.
- 22 S. Linic, P. Christopher and H. Xin, *Acc. Chem. Res.*, 2013, **46**, 1890–1899.
- 23 P. Christopher, H. Xin, A. Marimuthu and S. Linic, *Nat. Mater.*, 2012, **11**, 1044–1050.
- 24 M. T. Sun, Z. L. Zhang, L. Chen and H. X. Xu, *Adv. Optical Mater.*, 2013, **1**, 449–455.
- 25 M. T. Sun, Z. L. Zhang, L. Chen, S. X. Sheng and H. X. Xu, *Adv. Optical Mater.*, 2014, **2**, 74–80.
- 26 Z. L. Zhang, X. R. Tian, H. R. Zheng, H. X. Xu and M. T. Sun, *Plasmonics*, 2013, **8**(2), 523–527.
- 27 B. Ren, G. Picardi and B. Pettinger, *Rev. Sci. Instrum.*, 2004, **75**, 837–841.
- 28 P. C. Lee and D. Meisel, *J. Phys. Chem.*, 1982, **86**, 3391–3395.
- 29 P. Hohenberg and W. Kohn, *Phys. Rev. B: Condens. Matter Mater. Phys.*, 1964, **136**, B864–B871.
- 30 C. T. Lee, W. T. Yang and R. G. Parr, *Phys. Rev. B: Condens. Matter Mater. Phys.*, 1988, **37**, 785–789.
- 31 A. D. Becke, *J. Chem. Phys.*, 1993, **98**, 5648–5652.
- 32 P. J. Hay and W. R. Wadt, *J. Chem. Phys.*, 1985, **82**(1), 270–283.
- 33 M. J. Frisch, *et al.*, *Gaussian 09 Revision A. 02*, Gaussian Inc., Wallingford, CT, 2009.
- 34 H. J. Lee and W. Ho, *Science*, 1999, **286**, 1719–1722.
- 35 S. W. Hla and K. H. Rieder, *Annu. Rev. Phys. Chem.*, 2003, **54**, 307–330.
- 36 K. H. Kim, K. Watanabe, D. Mulugeta, H.-J. Freund and D. Menzel, *Phys. Rev. Lett.*, 2011, **107**, 047401, (1–4).